# 1

# General Introduction to Transmission Electron Microscopy (TEM)

**Peter Goodhew**
*School of Engineering, University of Liverpool, Liverpool, UK*



## 1.1 WHAT TEM OFFERS

Transmission electron microscopy is used to reveal sub-micrometre, internal fine structure in solids. Materials scientists tend to call this *microstructure* while bioscientists usually prefer the term *ultrastructure*. The amount and scale of the information which can be extracted by TEM depends critically on four parameters; the resolving power of the microscope (usually smaller than 0.3 nm); the energy spread of the electron beam (often several eV); the thickness of the specimen (almost always significantly less than 1 μm), and; the composition and stability of the specimen. The first and second of these depend largely on the depth of your pocket – the more you spend, the better the microscope parameters. The third is usually determined by your experimental skill while the last depends on luck or your choice of experimental system. The slim book by Goodhew *et al.* (Goodhew, Humphreys and Beanland,

*Aberration-Corrected Analytical Transmission Electron Microscopy*, First Edition.
Edited by Rik Brydson.

2001) gives a simple introduction to all types of electron microscopy, whilst the comprehensive text by Williams and Carter provides more detailed information on transmission electron microscopy (Williams and Carter, 2009).

The two available types of TEM – CTEM and STEM – differ principally in the way they address the specimen. The conventional TEM (CTEM) is a wide-beam technique, in which a close-to-parallel electron beam floods the whole area of interest and the image, formed by an imaging (objective) lens after the thin specimen from perhaps $10^6$ pixels, is collected in *parallel*. The scanning TEM (STEM) deploys a fine focused beam, formed by a probe forming lens before the thin specimen, to address each pixel in *series* as the probe is scanned across the specimen. Figure 1.1 summarises these differences. In both types of instrument analytical information from a small region is usually collected using a focused beam. The smallest region from which an analysis can be collected is defined by the diameter of this beam and hence the corresponding through-thickness volume in the specimen within which various inelastic scattering (energy-loss) processes take place.

As we will discuss in Chapter 2, the image resolution in CTEM is primarily determined by the imperfections or aberrations in the objective lens, whilst in a STEM instrument the resolution of the scanned image (as well as the analytical resolution described above) is determined largely by the beam diameter generated by the probe-forming lens which is also

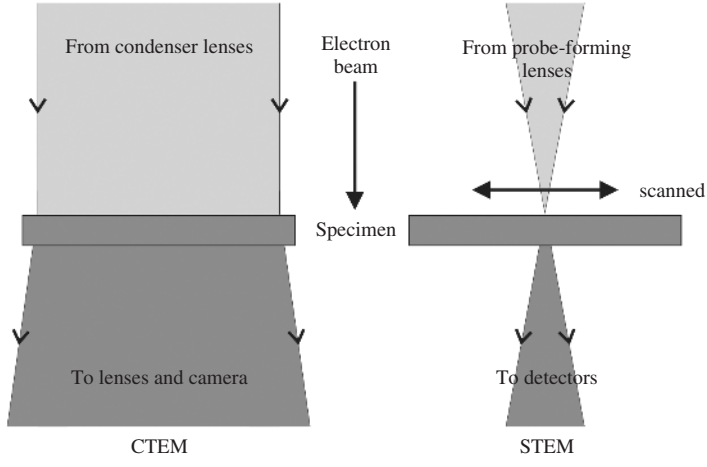


**Figure 1.1** The electron beam in CTEM and STEM instruments. Note that in many STEM instruments the beam actually travels upwards rather than down as shown here.

limited by aberrations. In recent years, technical difficulties have been overcome principally due to increases in computing power which have allowed both the diagnosis and correction of an increasing number of these lens aberrations (Hawkes, 2008). Aberration correction could in principle be applied to any magnetic lens in any microscope. However there are in practice two key areas where it is employed (in some cases in tandem): the condenser/illumination system and the objective lens. In STEM, of course, there is only a condenser system, which is better called a probe-forming lens (confusingly in a STEM this is often referred to as an objective lens – however, the important point is that it lies before the specimen) – making full aberration correction significantly cheaper! One of the main benefits of the correction of spherical aberration in STEM, is in the reduction of the 'beam tails' so that a fine beam positioned on a specified column of atoms does not 'spill' significant electron intensity into neighbouring columns. As we will see, this has big implications for the STEM-based techniques of high angle annular dark field (HAADF) or 'Z contrast' imaging and electron energy loss spectrometry (EELS) analysis (see section 1.3).

Although CTEM instruments far outnumber STEMs the advantages of the STEM approach – mainly the superior control over the positioning of the beam and better scope for detecting useful signals – are widely recognised and many CTEM instruments now include some STEM capabilities. At the present state of the art, aberration corrected STEM instruments probably offer the best (i.e. most sensitive and highest spatial resolution) analytical capabilities. Therefore, the primary focus of this handbook will be aberration correction in STEM, and Chapters 3–6 introduce and describe this approach in more detail. However aberration correction in CTEM is discussed for comparative purposes in Chapter 9.

All the potential ways in which imaging or analytical information can be extracted by any type of TEM depend critically on the interactions between the electrons in the beam and the electrons and/or nuclei of the atoms which comprise the specimen. We therefore consider some of the most useful interactions in the next section. As this text is, by design, somewhat brief, the description of these interactions is principally an introduction and further detail may be found in the extremely comprehensive text of Egerton (Egerton, 1996).

## 1.2 ELECTRON SCATTERING

Electron scattering within the specimen can be characterised in various ways. In what follows the *primary electron* is a single high energy electron

in the beam which (for TEM specimens of useful thickness) passes through the specimen, whilst a *secondary electron* is created within the specimen and might or might not subsequently leave the specimen.

Simplistically we refer to *elastic scattering*, implying that the energy lost by the primary electron is too small to be detected, or *inelastic scattering*, implying an energy loss big enough to be detected in the microscope. Staying at the simplistic level, we can say that elastic scattering occurs mainly from interactions with atomic nuclei (or the whole electrostatic field of the atom), is responsible for diffraction from crystalline specimens and is used to reveal structure; meanwhile inelastic scattering mainly involves electron-electron interactions and is mainly exploited for analysis – for example by EELS or energy dispersive X-ray (EDX) analysis, techniques which are discussed in Chapter 7.

A second way of characterising electron scattering is in terms of the process, that is what exactly happens or what is produced. Thus we can distinguish Rutherford or Compton scattering, plasmon or phonon production, ionization and several other processes (Egerton, 1996).

A third way of describing scattering within a specimen is to indicate the average number of scattering events of a specific type during the transit of a single primary electron. In this context *single scattering* implies that only one or two (or zero) events of the specified type are likely to occur during the passage of a single primary electron. *Plural scattering* then implies that a countable number of events occur, that is a sufficiently small number that Monte Carlo calculations (these are computer simulations based on probabilities of occurrence) might be able to keep track of them. Finally *multiple scattering* implies that the scattering events are so frequent that an almost uncountable number occur during the lifetime of the primary electron within the specimen. This is rare in a thin TEM specimen but is of great relevance to scanning electron microscopy (SEM) of (bulk) solids, when at some stage the primary electron loses most of its energy and becomes indistinguishable from any other electron in the specimen.

An important concept related to the frequency with which any particular interaction occurs is the *mean free path*, $\Lambda$, which is the average distance travelled by the primary electron between interactions. The same idea can be alternatively expressed by the *cross-section*, $\sigma$, the apparent cross-sectional area offered to the primary electron by the scattering entity. These two quantities are simply related via:

$$\Lambda = 1/(N_V \sigma) \tag{1.1}$$

where $N_V$ is the number of scatterers (atoms) per unit volume. The appropriate cross-section depends on the solid angular range, $\Omega$, over which the scattering is detected, so scattering probability is often referred to in terms of the differential cross-section $d\sigma/d\Omega$.

Electron interactions are sometimes characterised as spatially *coherent* (resulting in an in-phase effect such as diffraction from neighbouring scattering centres) or *incoherent* (not in phase, resulting in uncorrelated events from different scattering centres, such as high angle elastic scattering or the whole range of inelastic scattering events). It is important, however, to realise that in electron microscopy there is only one electron in the microscope at a time – at the currents commonly used, individual electrons are spaced perhaps a metre apart. The concept of coherence is therefore not easy to comprehend, and one hears statements of the type 'each electron can only be coherent with, and thus interfere with, itself.' Coherent electrons each 'make the same pattern'. In some circumstances it is also necessary to worry about *temporal* coherence, as well as *spatial* coherence. This is related to the variation in wavelength among the electrons and thus to the energy stability of the electron gun. Again it is conceptually difficult: coherence lengths are inversely proportional to the energy spread of the beam probe (which in STEM we usually try to keep below 1 eV) and they have magnitudes of the order of hundreds of nm. The conceptually difficult bit is that we are concerned about the temporal coherence, characterised by a length less than a $\mu$m, of electrons which are a metre or so apart and therefore at first sight independent and unaware of each other.

Finally, for the moment, we need to define the wave vector, $\mathbf{k}$, and scattering vector, $\mathbf{q}$. We will use the convention that $|\mathbf{k}| = 2\pi/\lambda$, rather than $1/\lambda$. If $\mathbf{k}$ is the incident wave vector and $\mathbf{k}'$ is the resultant scattered wave vector then the scattering vector is simply the difference between the two, $\mathbf{q} = \mathbf{k} - \mathbf{k}'$, as shown in Figure 1.2. Note here the direction of the scattering vector $\mathbf{q}$ is taken as that of momentum transfer *to* the specimen (equal to $h/2\pi$ times $\mathbf{q}$) which is opposite to the direction of the wavevector change of the fast electron.

In order to understand the range of potential analytical techniques available to the electron microscopist we need to understand a little about each of the more common (or more useful) interactions. To aid the subsequent description, Figure 1.3 displays a schematic spectrum of electron energies after their transmission through a thin specimen (in this case an EELS spectrum of calcium carbonate).

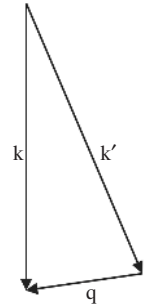


**Figure 1.2** Vector diagram of the incident and scattered wavevectors, **k** and **k′**. The corresponding scattering vector is **q**.

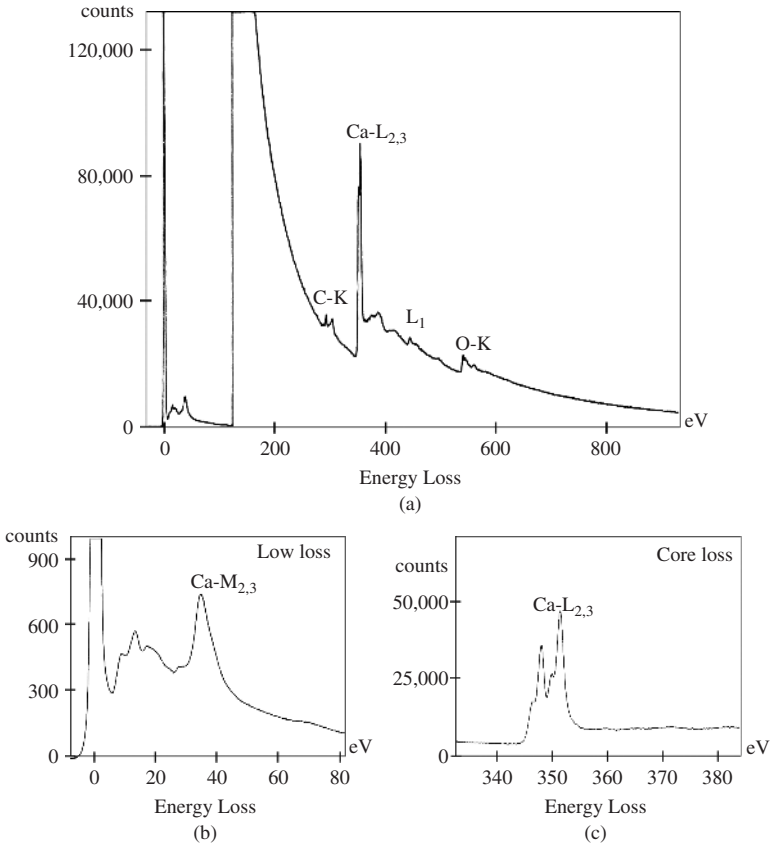


**Figure 1.3** Highly schematic Electron Energy Loss (EELS) spectrum of calcium carbonate showing the zero loss peak, a band gap, interband transitions, a plasmon peak (followed by a change in intensity scale) and ionisation edges: a carbon K-edge at ca. 285 eV, a calcium $L_{2,3}$ edge at ca. 350 eV and an oxygen K-edge at ca. 532 eV. Adapted from the *EELS Atlas* by C.C. Ahn and O.L. Krivanek.

### 1.2.1 Elastic Scattering

Elastic scattering involves no (detectable) energy loss and is represented by the peak at zero energy loss in Figure 1.3. It is usually described in terms of Rutherford scattering from an atom or ion. Introductory texts give the probability of scattering through an angle $\theta$ as $p(\theta) \propto 1/E_0^2 \sin^4(\theta/2)$, where $E_0$ is the electron (kinetic) energy. This expression implies strongly forward-peaked scattering in which the scattering is very much more likely to be through a very small angle. However, Rutherford scattering ignores screening of the nucleus by localised electrons and overestimates scattering at low angles. It also gives an infinite cross section if integrated over all angles! A better treatment leads to (Egerton, 1996):

$$d\sigma/d\Omega = 4\gamma^2 Z^2/a_0^2 q^4 \quad \text{where } q = |\mathbf{q}| = 2k \sin(\theta/2) \tag{1.2}$$

Here $\gamma$ (where $\gamma = [1 - v^2/c^2]^{-1/2}$) is the relativistic factor for the electron velocity ($v$) relative to the speed of light (c), Z is the atomic number, $a_0$ is the Bohr radius, q is the magnitude of the scattering vector and $k = |\mathbf{k}|$ is the magnitude of the wave vector of the incident electron ($k = 2\pi/\lambda$ for an electron of wavelength $\lambda$, as defined above). Screening can be taken care of by replacing $q^2$ by $q^2 + r_0^{-2}$ where $r_0$ is a screening radius. Here it is still the case that, at small angles, $d\sigma/d\Omega \propto 1/E_0^2(\theta/2)^4$ but now the magnitude of scattering is smaller and more realistic.

Low angle elastic scattering, because of its spatially coherent nature, can give information on the relative positions of atoms within the sample and is heavily exploited in diffraction techniques, both selected area and convergent beam, and (together with inelastic scattering) in the formation of Kikuchi bands. However, apart from HAADF imaging (see section 1.3 below) and some recent quantitative CBED developments, it is rare that elastic scattering intensities are measured or interpreted in electron microscopy, so inaccuracies in the Rutherford-based approach of the previous paragraph are usually not important.

An important point of terminology in terms of elastic scattering is the distinction between the kinematical and the dynamical scattering regimes. These terms refer to the approximations which it is appropriate to use. In a kinematical scattering regime each particle in the illuminating probe has only a small chance of being scattered, and the approximation can be made that the incoming probe loses negligible intensity. This is a reasonable approximation in many cases of X-ray and neutron scattering but is usually only a poor approximation for electrons passing through

a crystal owing to their large interaction with matter. In contrast, in the dynamical regime multiple scattering occurs, with multiple beams excited within the specimen which can then interfere. Intensity which oscillates with depth is then the norm for any beam.

Finally, an important concept in STEM is electron channelling, which is explored further in section 5.4. When the electron probe is located over an atomic column in a crystal, the electrons tend to be trapped by the attractive, periodic potential of the atoms. The process acts somewhat like a waveguide, and owing to the dynamical nature of the process, oscillations of the intensity of the wave on the atom sites with depth in the crystal are seen.

### 1.2.2 Inelastic Scattering

Most electron spectrometry associated with TEM involves measuring the energy of the primary electrons after they have passed through the specimen as displayed in Figure 1.3. Most such electrons have only lost less than a few tens of eV so are still highly energetic, typically around 100 keV or 200 keV. The spectrometers available to electron microscopists have a useful energy resolution limited to 0.1 eV or more in these circumstances, and the energy spread in the probe is likely to be at least 0.25 eV, so microscopists cannot easily avail themselves of processes with energy loss less than 1 eV or so. Thus, despite their numerical preponderance (arising from their short mean free path), inelastic scattering events leading to the production of *phonons* are not usefully exploited and are subsumed in the zero loss peak. Phonon scattering contributes to the background of images and diffraction patterns, and is ultimately responsible for heating the specimen, but because little can be deduced from its intensity or angular distribution it is rarely useful (at least at present). An effect which is in practice indistinguishable from phonon excitation (at least at room temperature) is thermal diffuse scattering (TDS), which is in effect the interaction of the probe electrons with pre-existing phonons. Both effects contribute to the background of many images, diffraction patterns and spectra, but the two effects cannot be separated unless the specimen is cooled, when TDS will be reduced while phonon excitation will not.

#### *1.2.2.1 Plasmon Scattering*

A plasmon is a collective oscillation of 'free' electrons induced by the transmission incident electron. As such it is rather a non-localised

scattering event occurring over a number of atomic sites. It dies away very quickly but dissipates significant energy, usually in the range up to 30 eV (Figure 1.3). Plasmon excitation can therefore be responsible for energy losses of tens of eV from a primary electron. The mean free path depends on the specimen but is typically in the 100 nm range. In specimens which are too thick for the most accurate or precise analysis, two or more plasmons can be excited by a single primary electron, leading to 'double' and 'triple' plasmon peaks in the EELS spectrum (section 7.4).

Plasmon-like oscillations occur even in non-metallic materials without apparent free electrons. Oscillations with different characteristic energies from bulk plasmons are also associated with surfaces and interfaces. All these phenomena are loosely referred to as plasmons. In the spectrum in Figure 1.3, it is apparent that plasmons generally overlap in energy with signals due to the transitions of single electrons between the outermost bands of electron energies. This combined valence electron scattering also contributes to the background of the EELS spectrum at higher energies which has considerable intensity at higher scattering angles.

Plasmon peaks are generally broad, with energies which are not uniquely representative of the specimen (unlike characteristic X-rays or Auger electrons, for instance). Egerton (1996) gives a list of measured and calculated values for many materials. They are a major and intense feature of EELS spectra, but since early attempts in the 1960s have only rarely been used for analysis, although recently small shifts in plasmon peak energies have been used to detect changes in composition and there is increasing interest in the excitation of plasmon modes in nanostructures.

#### *1.2.2.2 Inner Shell Ionisation*

The most useful, but not most frequently occurring, interaction is the ejection by the primary electron of a localised bound electron from a sample atom. The cross-section for the excitation of an inner shell electron is usually small (mean free paths are often $>1\,\mu m$) but the energy loss is often quite sharp and very characteristic of both the element and its state of bonding. Inner shell excitation is thus at the heart of energy loss spectrometry in the EM, leading to small but easily-recognised 'edges' in EEL spectra (Figure 1.3).

Following ionisation, the atoms of the specimen will relax, emitting either a characteristic X-ray (superimposed on a set of continuous background X-rays known as *Bremsstrahlung*) or an Auger electron.

X-rays are relatively easily detected in the column of a TEM and X-ray emission forms the basis of EDX analysis (see section 1.3). Auger electrons, on the other hand, require quite large spectrometers and because they are charged need sophisticated techniques to extract them from the microscope whilst preserving information about their energy. They are therefore rarely used for analysis in the TEM.

Inner shell excitations are dominated by the structure of the single atom, so are capable of being treated theoretically using simple models. Egerton (1996) and also Brydson (2001) give substantial detail of appropriate theories, the prediction of cross-sections, and the appearance of edges in an experimental spectrum. It is worth noting that significant information about the density of empty states and thus the bonding within the specimen can be deduced from near-edge fine structure (ELNES, at the start of the edge) and extended fine structure (EXELFS, after the main edge).

All these topics are examined in more detail in Chapter 7.

## 1.3 SIGNALS WHICH COULD BE COLLECTED

A 'standard' analytical CTEM is able to collect bright field and dark field images, selected area and convergent beam diffraction patterns, characteristic X-ray spectra (EDX) and electron energy loss (EEL) spectra. For an introduction to all of these, consult Goodhew *et al.* (2001). Here, we primarily focus on STEM.

A 'standard' STEM offers a similar set of possibilities, but differently optimised and set up for mapping. In addition it offers annular dark field (ADF) imaging. This is discussed further in Chapter 3, section 3.4. Bright field STEM images contain all the standard contrast mechanisms as experienced in bright field CTEM: mass-thickness, diffraction and phase contrast (Goodhew *et al.*, 2001). Of particular interest to users of aberration-corrected instruments is high-angle annular dark field (HAADF) imaging. High-angle in this context signifies several tens of mrad, which is beyond the angle at which diffraction maxima (spots) of any significant intensity are found. High-angle scattered electrons are few in number, and mostly result from Rutherford scattering. Their great advantage for imaging and analysis is that they are usually insensitive to structure and orientation but strongly dependant on atomic number, with the intensity varying as $Z^{\zeta}$ where $\zeta$ lies between 1.5 and 2 and is often quoted for most experimental setups as being around 1.7. A HAADF image, collected from electrons scattered in the angular range

perhaps 50 to 200 mrad, therefore has a local intensity which strongly depends on composition, but depends less strongly on structure or precise orientation. If the specimen is uniformly thick in the area of interest the HAADF intensity can be directly related to the average atomic number in the column at each pixel. If the beam is less than one atom dimension in diameter, for instance in an aberration-corrected STEM, then atom column compositional resolution is therefore possible (strictly if we have strong channelling of the probe). This is discussed further in Chapters 5 and 6.

An energy-filtering microscope is one in which the image (or indeed the diffraction pattern) can be formed using electrons whose energy has been selected after they have passed through the specimen. This is achievable in a CTEM with an in-column 'omega filter' or post-column imaging filter (Brydson, 2001) or, more elegantly, in STEM by so-called *spectrum imaging*. In this technique an EELS spectrum is collected at each pixel. The image intensity at each pixel is measured during post processing from a defined energy-loss range within the appropriate spectrum. This effectively produces compositional maps of the specimen, although, as discussed in Chapter 7, care must be taken to select an appropriate energy range and background subtraction routines.

It has been implicitly assumed in this chapter that EELS is the analytical method of choice for high resolution microscopy. There are two key reasons for this dominance; firstly the EELS spectrometer can be located far from the specimen and thus does not interfere with the important region around the specimen, which is already crowded with lens pole pieces and specimen tilting apparatus. Secondly, electrons can be collected by an EELS spectrometer with almost 100% efficiency, so little useful signal is lost.

Despite the advantages of EELS, analysis using characteristic X-rays (EDX) is also widely available. Relaxation of excited atoms by emission of an X-ray becomes more efficient for heavier atoms and EDX might be the analytical technique of choice for specimens containing heavy atoms (say $Z > 30$). However because X-rays cannot be deflected into an appropriate detector their collection will always be inefficient (usually less than 1%) and signal strength will always be a problem from a thin specimen. Both EELS and EDX are more fully discussed in Chapter 7. Other potential, but relatively unexploited techniques applicable to STEM are discussed at the end of section 3.4.

For any signal from a specific feature within a TEM specimen, in order to detect or 'see' it in an image the contrast (strictly defined as $\{S_F - S_B\}/S_B$ where $S_F$ and $S_B$ are the signals from the feature and

the surrounding background respectively) needs to be greater (usually between three and five times greater) than the inherent noise level in the background signal, which in Poisson statistics is the square root of the number of counts. Thus detection and visualisation of a feature is highly dependent not only on the resolution but also critically depends on the contrast.

## 1.4 IMAGE COMPUTING

Most of the easy problems available to the microscopist have already been addressed during those halcyon days when a qualitative argument (sometimes even just hand-waving) was sufficient to explain new features in a micrograph. Many of today's more sophisticated questions can only be answered by a sophisticated analysis of the process of image formation, together with sympathetic processing of experimental images and spectra. Both CTEM and STEM are thus supported by suites of programs designed to manipulate experimental images ('image processing') and to predict what the image of a possible structure would look like in the microscope ('image simulation').

### 1.4.1 Image Processing

Since image collection (recording) is now almost universally digital, images at any resolution are typically stored as $1024 \times 1024$ (for example) datasets, giving about $10^6$ image pixels per image. Such images can be manipulated (almost too easily) in a variety of ways. In the future microscopists will no doubt use clever recognition algorithms to locate features of interest and automatically select them for further study, but at present the principal processing techniques (beyond simple control of brightness and contrast) are based around fast Fourier transforms (FFTs) of the image. For images containing a large degree of periodicity (e.g. crystalline materials) such transforms (power spectra corresponding, of course, to diffraction patterns of the same area of the specimen) can be used to filter out 'noise' before back-transformation into a 'better' image. Commercial programs such as Digital Micrograph (Gatan Inc. – www.gatan.com) do this sort of thing, and a lot more, extremely efficiently. However the microscopist must always be aware of the potential for introducing artefacts during what might all too easily be used as 'black box' processing.

Image processing can be used to extract, or sometimes just to make more evident, specifically interesting features of an image. To be applied, it requires little or no *a priori* understanding of the nature of the specimen and typically needs no input parameters.

There is increasingly an ethical issue associated with publishing both analytical and image data from EMs. Although it takes more space (on paper or on-line) we would recommend that the raw data is always published, as well as any processed version of it which might be easier to interpret. Any publication should also make precisely clear what processing has been applied to any image or spectrum. Putting the raw data in the public domain ensures that conclusions can be checked by other researchers.

### 1.4.2 Image Simulation

Image simulation has been used for many decades and in the 1960s simple programs were in use to predict the appearance of isolated dislocations in thin crystals, with the background assumed to be a diffracting continuum. However the increasing resolving power of modern microscopes has shifted the focus of simulation towards atomic column resolution and structural images. Simulated images can not only help to 'solve' structures but they can also assist the microscopist to distinguish specimen features from instrumental artefacts. They will be referred to later in this book in Chapters 5, 8 and 9.

The simulation of high resolution EM images can only be undertaken, at the present time, by a process in which the microscopist constructs a possible arrangement of atoms and then asks the question 'what would this look like in my microscope under the operating conditions I think I am using?'. Comparison with an actual experimental image is then usually, but not necessarily, performed by eye, to answer the question 'is this what my image shows?'. The further important question 'is this the only structure which might look like this in the microscope?' is, regrettably, not always fully addressed or addressable!

In contrast to image processing, image simulation requires the input of a large number of pieces of information. Programs such as QSTEM (Koch, 2002), TEMSIM (Kirkland, 1998) or JEMS (Stadelmann, 1987), some of which are available as freeware, typically expect the user to define the location and atomic number of every atom in the test structure, the local specimen thickness, the electron energy, the exact value of

defocus, the size of apertures, the shape (profile) of the beam (influenced by lens aberrations), atomic scattering factors and the orientation of the specimen. Several of these parameters are very difficult to measure accurately, so simulations are often run for a range of thicknesses and a range of defoci, while the corresponding experimental images are collected as a through-focal series. Despite this complexity many structures have been solved or confirmed by the use of such simulations.

High resolution simulations, for CTEM or STEM, adopt one of two approaches, based on Bloch wave propagation or the multislice principle. Because Bloch wave calculations require greater processing power, and are in some ways less flexible, multislice programs now dominate the field. The principle of a multislice calculation is to cut the trial structure into thin slices perpendicular to the electron beam and compute, for each slice in turn, its effect on the phase of the slowly-varying part of the electron wave function. The wave is then propagated to the next slice. Under appropriate conditions the effects of each slice can be added and the wave propagating from the bottom of the specimen is effectively the image. For the case of CTEM images, the incident wave is simply described as a plane wave, whilst the simulation of images for STEM is discussed in more detail in section 5.6 and some examples are provided in Chapter 8.

## 1.5 REQUIREMENTS OF A SPECIMEN

A specimen suitable for study by TEM should obviously be thin enough for electron transmission, and representative of the material about which we wish to draw conclusions. These simple requirements imply that in most cases we must prepare a thin specimen from a larger sample, and in all cases we must assure ourselves that the processes of preparation, mounting and examination do not change, in any uncontrolled way, the important features of the specimen.

For high resolution studies, whether imaging or analysis, the constraints are more severe. The ideal specimen must be thin enough that:

- it can be treated as a weak phase object (see below);
- electron beam spreading within the specimen is negligible;
- (if a nano-particle) it can be supported on a thin substrate with the total thickness still small enough to satisfy the two constraints listed above;

. . . but also thick enough that:

- it is self-supporting over a region large enough to find the features of interest
- its two surfaces are far enough apart that the material within remains characteristic of the bulk (unless, of course, it is the surfaces in which you are interested)
- surface contamination does not dominate the signal
- there is sufficient signal from scattering events to give statistically significant (i.e. low noise or high enough signal to noise ratio) images or spectra.

These requirements imply that, for most materials to be imaged or analysed at atomic-column resolution, the appropriate thickness will lie in the range up to 50 nm.

It would also be helpful if specimens prepared from the bulk could be perfectly flat and parallel-sided with no contamination or surface amorphised layer, while nano-particles could be of regular shape (so that their thickness is calculable from their projected shape and size). Every specimen should resist both ionization damage and displacement damage by the primary beam.

Almost no real specimens meet all these criteria, but the list of ideal properties should always be borne in mind. Three of the requirements merit some further more quantitative consideration.

A *weak phase object* is a specimen so thin that the electron beam passing thorough it only suffers a modest phase shift, while its amplitude remains effectively unchanged. The approximation that a specimen is indeed a weak phase object is important for much of the treatment in Chapter 5. It should be obvious that such a specimen must be substantially thinner than the mean free path for all the inelastic scattering processes. In practice many biological specimens will meet this criterion at thicknesses below 50 nm, but specimens containing substantially heavier atoms would need to be much thinner.

Beam spreading in a specimen of thickness $t$ is difficult to calculate if multiple scattering is involved, but for specimens which are thin enough to act as weak phase objects and in which single scattering is a good assumption, the beam spreading, b, can be estimated using an equation such as (Goldstein *et al.*, 2003)

$$b = 7.2 \times 10^5 \cdot (Z/E_o) \cdot (\rho/A)^{0.5} \cdot t^{1.5} \qquad (1.3)$$

where $E_0$ is the electron beam energy in keV, $\rho$ the density in g/cm$^3$ and Z and A are the atomic number and atomic weight respectively; note that b and t are in cm. You will find that beam broadening is small in a weak phase object but it is worth remembering that for atom column resolution it only requires a broadening of 0.2 nm to take a significant fraction of the beam intensity to the next atom columns. Bear in mind that most specimens are actually thicker than the weak phase object regime, and that beam spreading would be greater than implied by the Goldstein approach. However Goldstein accounts for electrons scattered in all directions, each of which could excite an X-ray. Not all of these electrons could enter an EELS spectrometer, so for EELS the equation might overestimate beam broadening. Strengthening what was said at the beginning of the paragraph, beam spreading is difficult to estimate, never mind calculate!

For a given incident beam energy, beam damage of the specimen is generally a function of the electron fluence (i.e the total number of electrons incident per unit area of specimen) and hence energy deposited within the specimen volume (known as dose); in some cases the fluence rate (usually quoted in current per unit area) can be important. There is some confusion in the literature about these terms; you are advised to read and consider the units of these quantities carefully. Beam damage of the specimen can occur by two dominant mechanisms – knock-on damage in which an atom or ion is displaced from its normal site, and ionisation damage (in some contexts called radiolysis) in which electrons are perturbed leading to chemical and then possibly structural changes. Both mechanisms are discussed by Williams and Carter (2009) and also Egerton *et al.* (2004), who give a chart showing the ranges of primary beam energy which are likely to cause displacement damage for specific atomic species.

Both types of damage are very difficult to predict or quantify with accuracy, because they depend on the bonding environment of the atoms in the specimen. However, in most circumstances, the knock-on cross-section increases with primary beam energy, while the ionisation cross-section decreases. There is thus a compromise to be struck for each specimen to find a beam energy which is low enough not to cause significant atomic displacement but is high enough to suppress too much radiolysis. We return to the subject of beam damage in STEM in section 3.5.

There is no right answer to the choice of specimen thickness or beam energy. Many microscopists only have easy access to a limited range of beam energies and struggle to prepare a good thin specimen, so in

practice microscopy involves looking around the specimen for a 'good thin region' and studying it with 100 keV or 200 keV electrons. In the future more consideration may be given to the choice of optimum beam energy, but this requires that the alignment of the microscope and any ancillary equipment such as an EELS spectrometer at any keV be a quick and simple procedure – which it usually is not.

## 1.6 STEM VERSUS CTEM

There are some advantages to the use of STEM imaging, rather than CTEM. It should be obvious that the STEM configuration is ideal for performing analyses point by point at high sensitivity using multiple signals, and indeed this fact forms the basis for this whole book.

Additionally it should also be apparent that, assuming the signal collection efficiency in STEM is optimised or multiple STEM signals are simultaneously acquired, the total electron fluence or dose which must be delivered to a specimen pixel to generate a specified signal-to-noise ratio (whether for an image or an analytical spectrum) is the same whether delivered by CTEM or STEM. However the dose in STEM is delivered over a short period, which is followed by a longer period of relaxation, whereas in CTEM the instantaneous dose rate is much lower but the dose is continuous. These do not necessarily lead to the same damage, particularly if specimen heating is involved; here the perceived wisdom is that local heating is less for a focused STEM probe than for broad beam CTEM owing to the increased diffusion of thermal energy into surrounding, un-illuminated, cold areas. There is also the possibility, using digital STEM, of positioning the beam consecutively on pixels which are not adjacent – i.e. sampling periodically rather than flooding the whole area. This too can reduce damage at each pixel.

## 1.7 TWO DIMENSIONAL AND THREE DIMENSIONAL INFORMATION

TEM is a transmission technique and by its very nature produces a two dimensional projection of the interaction of the electron beam with the specimen, whether that be a projected image, a diffraction pattern down a particular crystallographic direction or an analytical signal from a projected through-thickness volume of the specimen. However, in microscopy in general, there is increasing interest in the determination of three dimensional information – known as tomography.

Electron tomography using both CTEM and STEM can be achieved by recording (usually) images for a number of different projections of the specimen and then recombining these images mathematically to form a three dimensional representation of the specimen. This may be achieved in one of three ways: the first, known as *tilt tomography*, is to actually tilt the specimen, usually incrementally but in some cases down certain directions, and record a set of images; the second method assumes that a set of separated objects (e.g. particles dispersed on a TEM support film) are all identical but are arranged over all possible orientations with respect to the direction of the electron beam and is known as *single particle analysis*. The final method known as *confocal electron microscopy* restricts the depth of field/focus in the image to a very thin plane using some form of confocal aperture before the image plane; a set of images are then recorded over a range of defocus and these are combined to give the three dimensional specimen. Chapter 8 gives some recent examples of such STEM tomography and indicates where aberration correction has made a substantial impact.

In conclusion, this initial chapter has both introduced and highlighted some of the important classifications and background theory as well as some of the key issues and developments for TEM in general. As mentioned earlier, the purpose of this handbook, and hence the following chapters, is to focus primarily on the benefits of aberration correction for the formation of smaller electron probes and hence, it will primarily focus on analytical electron microscopy and therefore STEM. However, aberration correction within the context of CTEM is discussed for comparative purposes in Chapter 9.

## REFERENCES

Brydson, R. (2001) *Electron Energy Loss Spectroscopy*, Bios, Oxford.

Egerton, R.F. (1996) *Electron Energy Loss Spectroscopy in the Electron Microscope*, Plenum Press: New York.

Egerton, R.F. Li, P. and Malac, M. (2004) Radiation damage in the TEM and SEM, *Micron* 35, 399–409.

Goldstein, J. Newbury, D.E., Joy, D.C., Lyman, C.E., Echlin, P., Lifshin, E., Sawyer, L. and Michael, J.R. (2003) *Scanning Electron Microscopy and X-ray Microanalysis*, Springer.

Goodhew, P.J., Humphreys, F.J. and Beanland, R. (2001) *Electron Microscopy and Analysis*. Taylor and Francis.

Hawkes, P.W. (ed.) (2008) *Advances in Imaging and Electron Physics*, Vol. 153, Elsevier.

Kirkland, E.J. (1998) *Advanced Computing in Electron Microscopy*, Plenum Press, New York.

Koch, C.T. (2002) Determination Of Core Structure Periodicity And Point Defect Density Along Dislocations, PhD Thesis, Arizona State University.
See also http://www.christophtkoch.com/stem/index.html

Stadelmann, P.A. (1987) EMS – A Software Package for Electron Diffraction Analysis and HREM Image Simulation in Materials Science, *Ultramicroscopy* 21: 131–146.
See also http://cimewww.epfl.ch/people/stadelmann/jemsWebSite/jems.html

Williams, D.B. and Carter, C.B. (2009) *Transmission Electron Microscopy: A Textbook for Materials*, Springer.